

Dynamic mechanism of the velocity splitting of ablated particles produced by pulsed-laser deposition in an inert gas

This content has been downloaded from IOPscience. Please scroll down to see the full text.

2011 EPL 96 55002

(<http://iopscience.iop.org/0295-5075/96/5/55002>)

View [the table of contents for this issue](#), or go to the [journal homepage](#) for more

Download details:

IP Address: 129.93.16.3

This content was downloaded on 10/09/2015 at 13:16

Please note that [terms and conditions apply](#).

Dynamic mechanism of the velocity splitting of ablated particles produced by pulsed-laser deposition in an inert gas

X. C. DING¹, Y. L. WANG^{1(a)}, L. Z. CHU¹, Z. C. DENG¹, W. H. LIANG¹, I. I. A. GALALALDEEN^{1,2}
and G. S. FU^{1(b)}

¹ College of Physics Science and Technology, Hebei University - Baoding 071002, PRC

² Faculty of Engineering and Technology, University of Gezira - Wad Madani, P.O. Box 20, Sudan

received 31 August 2011; accepted in final form 17 October 2011

published online 22 November 2011

PACS 52.38.Mf – Laser ablation

PACS 52.25.Fi – Transport properties

Abstract – The transport dynamics of ablated particles produced by pulsed-laser deposition in an inert gas is investigated via the Monte Carlo simulation method. The splitting mechanism of ablated particles is discussed by tracking every ablated particle with their forces, velocities and locations. The force analysis demonstrates that whether the splitting appears or not is decided by the releasing way of the driving force acting on the ablated particles. The “average” drag force, which is related to the mass and radius of the ambient gas, determines the releasing way of the driving force. Our simulated results are approximately in agreement with the previous experimental data.

Copyright © EPLA, 2011

Introduction. – Pulsed-laser deposition (PLD), one of the most popular fabrication methods for preparing nanoparticles of a variety of materials, has been receiving more and more attention due to its unique advantages, such as rapid thermogenic speed and small surface contamination [1–3]. As other preparation methods, the controllable preparation of nanoparticles with the designed size-distribution is expected for PLD. Only when nanoparticle formation dynamics is clarified, can we obtain the nanoparticles we want. As well known, nucleation and growth are always two crucial processes during the nanoparticle formation. Moreover, the nucleation occurs in the region in which the ablated particles possess the supersaturated density and the appropriate velocity/temperature, and the growth stops when these conditions cannot be met [4,5]. The temporal and spatial distribution dispersions of density and velocity of ablated particles induce the complexity of quantitatively investigating the nucleation and growth conditions during PLD. As one of important dispersions, the velocity splitting of the ablated particles, in which the plume splits into the distinct slow and fast components, has been paid more attentions [6–8] also because the fast component may affect its microstructure and even damage the growing material. The experimental results showed that

this phenomenon appears in a range between the target and the substrate when the laser fluence is higher than a critical value and the pressure is appropriate for an ambient species. Regarding the splitting dynamic mechanism, Dixon and Seely contributed it to the collision interaction like resonance charge transfer based on their observed data for carbon species in helium (He) gas [9]. Moreover, for the same system, Harilal *et al.* proposed that the fast and slow components are produced by two-body or many-body combination and the dissociation of larger clusters [10], respectively. Wood *et al.* analyzed systematically the plume splitting of silicon (Si) in He or argon (Ar) gas using combination of multiple elastic scatterings and hydrodynamic formulations [6]. There is the distinct discrepancy, however, between the simulated results on the current flux *vs.* time and their experimental data. This macroscopic model can not be used to trace each ablated particle, which results in the difficulty to search for the origin of the velocity splitting.

In this paper, we utilize a three-dimensional Monte Carlo simulation [11–13] to investigate the dynamic mechanism of velocity splitting of the ablated Si particles in an inert ambient gas.

Monte Carlo simulated details. – The PLD process can be classified into three separate regimes: 1) interaction of laser beam with the Si-target material resulting in evaporation of the surface layers and ejection of the

^(a)E-mail: hdwangyl@mail.hbu.edu.cn

^(b)E-mail: fugs@mail.hbu.edu.cn

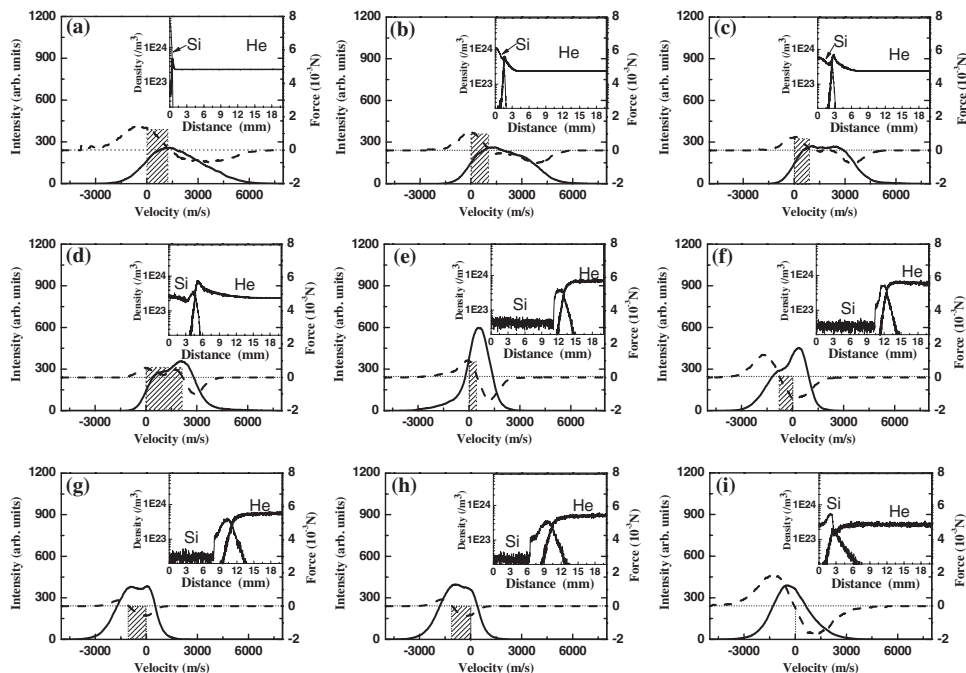


Fig. 1: Time evolution of the radial velocity distribution (the solid lines) and of the force distribution (the dashed lines) of the ablated particles. Where (a), (b), (c), (d), (e), (f), (g), (h) and (i) correspond to $0.1 \mu\text{s}$, $0.4 \mu\text{s}$, $0.7 \mu\text{s}$, $1.5 \mu\text{s}$, $8.0 \mu\text{s}$, $10.0 \mu\text{s}$, $12.0 \mu\text{s}$, $12.8 \mu\text{s}$ and $19.0 \mu\text{s}$, respectively. The inset shows the time evolution of the density distribution of the ablated particles (the solid line) and the helium ambient gas (the dotted line).

ablated particles (Si atoms and so on), 2) transport of ablated particles in an inert gas resulting in formation of nanoparticles, and 3) diffusion of as-formed nanoparticles with rather low kinetic energy resulting in deposition of thin films on the substrate. We focus on the second regime because the splitting produces during this regime. Some assumptions are adopted in our simulation: 1) The ablated particle possesses the same mass as Si atom: 2) The initial time corresponds to that the ablated particles just leave out the edge of Knudsen layer. The flux of the ablated particles usually constructs a conical shape of which the apex is cut with the laser spot diameter [14]. However, the experimental measurement usually generates a time delay of a few nanoseconds. Our initial time is earlier than the first image in the experiment. At that time the ablated particles are uniformly distributed within a cylindrical space of the laser spot diameter. The initial velocities of the ablated particles are satisfied with Maxwell-Boltzmann distribution [15]. 3) The ablated particles and the ambient atoms can interact as elastic hard-sphere scattering with a total collision cross-section σ_{ab} , which is independent of the scattering angle and $\sigma_{ab} = \pi(r_a + r_b)^2$, where r_a and r_b are the radii of the colliding particles. The post-velocities of the colliding particles is written with conservation of momentum and energy as,

$$\vec{V}'_a = \vec{c}_m + m_b / (m_a + m_b) \vec{c}'_r, \quad (1)$$

$$\vec{V}'_b = \vec{c}_m + m_a / (m_a + m_b) \vec{c}'_r, \quad (2)$$

in which

$$\vec{c}'_r = \vec{c}_r [(\sin \theta \cos \alpha) \hat{x} + (\sin \theta \sin \alpha) \hat{y} + \cos \theta \hat{z}], \quad (3)$$

where θ is the scattering angle from 0 to π , and α is obtained from a uniform distribution in the range of 0 to 2π ; \vec{c}_r and \vec{c}'_r are the relative velocities before and after a collision, respectively, \vec{c}_m is the velocity of centre of mass of a pair of colliding particles.

During the simulation, the velocities and locations of all ablated particles and all ambient atoms are recorded. According to Newton theorem,

$$\vec{F} = d\vec{p}/dt, \quad (4)$$

the force acting on each ablated particle is calculated. The statistics of the force and velocity distributions of ablated particles are calculated with velocity region width of 10 m/s.

Dynamic mechanism of splitting. – We consider the ablation of Si target in He/Ar gases with the constant pressure of 1000 Pa by using a KrF excimer laser with the laser fluence of 3.0 J/cm^2 , wavelength of 248 nm, and pulse duration of 15 ns. A substrate is placed at 2 cm distance from the Si target. When the ablated particles are just out the Knudsen layer, the density, the radial velocity and the total number of ablated particles are $1.66 \times 10^{26} \text{ m}^{-3}$, 1760 m/s and 1.01×10^{15} , respectively [12]. The time evolution of the radial velocity distribution of the ablated particles in He gas is shown as the solid lines in fig. 1, in which (a), (b), (c), (d), (e), (f), (g), (h) and (i) correspond to the results of $0.1 \mu\text{s}$, $0.4 \mu\text{s}$, $0.7 \mu\text{s}$, $1.5 \mu\text{s}$, $8.0 \mu\text{s}$, $10.0 \mu\text{s}$, $12.0 \mu\text{s}$, $12.8 \mu\text{s}$ and $19.0 \mu\text{s}$, respectively. The non-consistent time separation is chosen to emphasize the changing detail near to the critical time. Obviously,

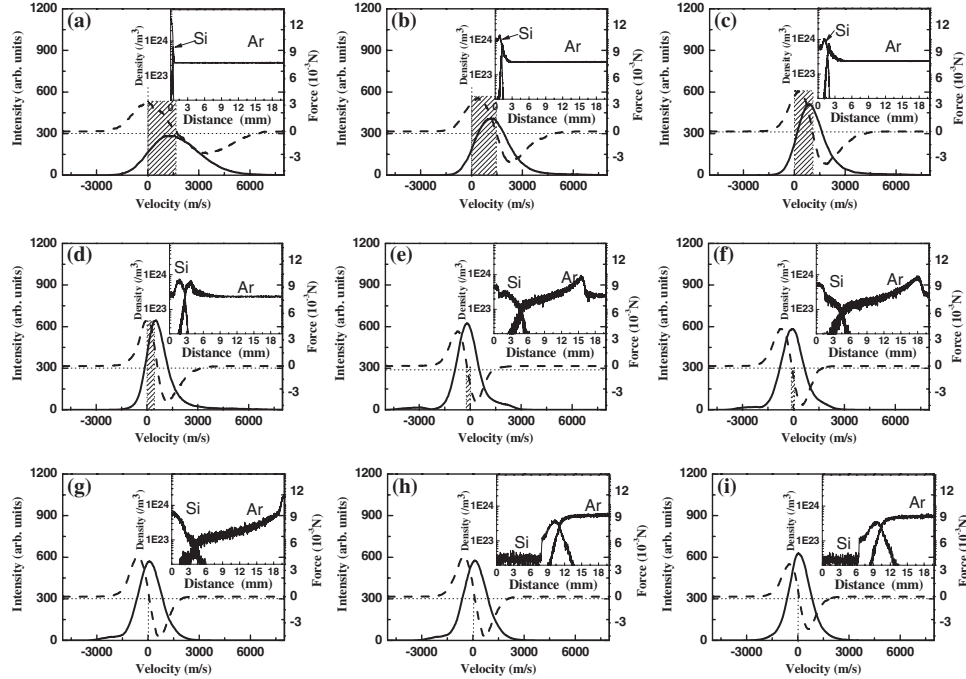


Fig. 2: Time evolution of the radial velocity distribution (the solid lines) and of the force distribution (the dashed lines) of the ablated particles. Where (a), (b), (c), (d), (e), (f), (g), (h) and (i) correspond to $0.1 \mu\text{s}$, $0.4 \mu\text{s}$, $0.7 \mu\text{s}$, $1.5 \mu\text{s}$, $8.0 \mu\text{s}$, $10.0 \mu\text{s}$, $12.0 \mu\text{s}$, $12.8 \mu\text{s}$ and $19.0 \mu\text{s}$, respectively. The inset shows the time evolution of the density distribution of the ablated particles (the solid line) and the argon ambient gas (the dotted line).

the velocity splitting is observed at $0.4 \mu\text{s}$, $0.7 \mu\text{s}$, $1.5 \mu\text{s}$, $10.0 \mu\text{s}$, $12.0 \mu\text{s}$ and $12.8 \mu\text{s}$, namely, the intensity-velocity curves possess two evident inflexions. The velocity distribution undergoes two cycles of emerging, sustaining and vanishing of splitting. Although the velocity distribution range and peak intensity change with the increase of time, the integrated area of the velocity distribution curve is constant because the total number of ablated particles is conservational. For each splitting cycle, one component always increases while the other one decreases gradually. At $\sim 0.7 \mu\text{s}/12 \mu\text{s}$, the two components possess the same peak intensities. And then the two peaks close with each other gradually and incorporate into a sole peak finally, namely, the splitting disappears. Under the above parameters, the results corresponding to Ar gas are shown as the solid lines in fig. 2, in which (a), (b), (c), (d), (e), (f), (g), (h) and (i) correspond to the results of $0.1 \mu\text{s}$, $0.4 \mu\text{s}$, $0.7 \mu\text{s}$, $1.5 \mu\text{s}$, $8.0 \mu\text{s}$, $10.0 \mu\text{s}$, $12.0 \mu\text{s}$, $12.8 \mu\text{s}$ and $19.0 \mu\text{s}$, respectively. Surprisingly, no splitting phenomenon is observed for Ar gas of 1000 Pa . Note a common knowledge that the external force is the essential origin induced the change of velocity. In order to search for the origin of the velocity splitting, the force distribution exerting on the ablated particles with the same velocity segment provided by the collisions with other particles is calculated by tracing the ablated particle with the information of velocity, as appended in the dashed lines of fig. 1 and fig. 2. The two dotted lines with zero velocity and zero force are plotted in the figures to clearly analyze the sign of the force meaning drive or drag. The shadowed region displays the velocity

section of the driving force. Figure 1 seems to demonstrate that the driving force can induce the splitting; however, fig. 2 indicates that the existence of driving force for some particles is necessary but not enough for the velocity splitting. For each cycle of splitting in He gas, the driving range in the force distribution first widens to its maximum, narrows gradually, and then finally becomes zero accompanied by the emerging, distinctness and vanishing of velocity splitting. Differently, the driving range under Ar gas decreases monotonously. From the varying detail of the force with velocity, we know that the splitting is absent when the positive force pointing to the substrate is antisymmetric with the minus force pointing to the target and the force antisymmetric point possesses the same velocity as intensity peak. A lot of particles with the same velocity are called as “group”. For He as ambient gas, at the time less than $0.4 \mu\text{s}$, the group containing most of the particles is force-free, while the slow groups including the particles moving towards to the target and the fast groups are compressed in velocity. Similarly, the ambient gas is compressed gradually to form a high-density peak in the front of interface and a shock peak in the background of the ambient gas. At $0.4 \mu\text{s}$, these two density peaks induce two maximum of minus force so that splitting appears. The time evolution of the radial density distribution of the ablated particles (solid lines) and the He/Ar ambient gas (dotted lines) is shown in the insets of fig. 1 and fig. 2.

At the initial stage, the particles with negative velocity are rebounded by the Si target and give the impetus to the particles with positive and low velocity, thus the particles

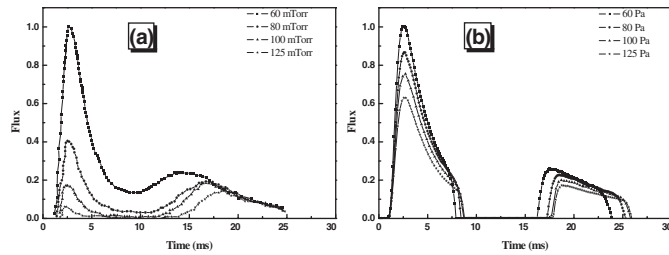


Fig. 3: The theoretical results (a) and experimental data (b) about the flux produced by laser ablation in argon gas.

with negative velocity become less and less. As the Si vapor expands and the He gas is compressed gradually, a high-density peak appears at the forefront of the He gas density, inducing two drags by ambient atoms or other ablated particles, thus two velocity groups are formed, which is the essential origin of the velocity splitting for the particles moving towards to the substrate. Surely, the ambient atoms entering into the Si vapor are rebounded by Si particles and provide an impetus to Si particles located at its front, thus the particles with positive and low velocity are acted by two-behavior impetus, and so the peak corresponding to the faster group increases. When the high-density peak of Si gets to its nearest position from the substrate, the compressed ambient gas possesses constant density distribution, thus the splitting disappears.

Whether the velocity splitting appears or not is decided by the releasing way of the driving force. When the experimental parameters are appropriate, the driving range presents monotonous or oscillatory decrease. The former cannot observe splitting, while the latter can induce the splitting. The observation time of the splitting depends on the antisymmetry of positive and negative forces.

The environment provides the drag force for the ablated particles, which varies with the time and position. In “average” meaning, the “average” drag force determines the releasing way of the driving force. When the “average” drag force is smaller, the releasing way of the driving force presents oscillatory decrease due to the underdamping. For the bigger drag force, monotonous decrease as overdamping. According to Yoshida’s model [16], the damping coefficient is in proportion to the ambient gas density. For the ambient gas (*e.g.*, Ar) with heavier atom, the lower pressure can induce the higher drag force, thus “monotonous decreasing” releasing of driving force, and therefore, no splitting takes place.

Comparison with the previous theoretical and experimental results. – The velocity splitting of ablated particles has been investigated experimentally and theoretically by Wood *et al.* [6], the experimental data of flux for Ar of 60 mTorr, 80 mTorr, 100 mTorr and 125 mTorr are copied in fig. 3(a) and the theoretical results are omitted. Figure 3(b) displays the corresponding results obtained by our model, which are in agreement with the

theoretical results of Wood (see ref. [6]). Compared with fig. 3(a), our model, as their theory, presents the distinct discrepancy with their experimental data. Concretely, the drop rate of flux as the increase of pressure in our calculation is less than that in the experiments, and the flux decreases to zero between two peaks in the calculated curves, which may be attributed to the absence of the nucleation and growth of Si nanoparticles. Additionally, the pressure of 60 Pa, 80 Pa, 100 Pa, 125 Pa is used in our model in order to compare with the experimental data.

Conclusion. – The dynamism of velocity splitting of the ablated particles produced by pulsed-laser deposition is investigated via Monte Carlo simulation. Whether the velocity splitting is observed or not decided by the releasing way of the driving force. If the velocity range of the driving force of the ablated particles obviously decreases with oscillation, the splitting is likely to be observed; otherwise, it cannot be observed. The releasing way of the driving force is decided by the “average” drag force of ambient gas. Our calculated data are approximately in agreement with the experimental result in the previous literature.

The authors are grateful for the financial support by the 973 program (2011CB612305), National Science Foundation of China (NSFC) (10774036), the NSF of Hebei Province (E2008000631) and foundation of Hebei University. Support from the Hebei Key Laboratory of Optic-electronic Information & Materials is also acknowledged.

REFERENCES

- [1] LOWNDS D. H., GEOHEGAN D. B., PURETZKY A. A., NORTON D. P. and ROULEAU C. M., *Science*, **273** (1996) 898.
- [2] PHARK S. H., CHANG Y. J. and NOH T. W., *Phys. Rev. B*, **80** (2009) 035426.
- [3] WANG Y. L., CHEN C., DING X. C., CHU L. Z., DENG Z. C., LIANG W. H. and FU G. S., *Laser Part. Beams*, **29** (2011) 105.
- [4] SCHRADER M., VIRNAU P. and BINDER K., *Phys. Rev. E*, **79** (2009) 061104.
- [5] TERSOFF J., JESSON D. E. and TANG W. X., *Phys. Rev. Lett.*, **105** (2010) 035702.
- [6] WOOD R. F., CHEN K. R., LEBOEUF J. N., PURETZKY A. A. and GEOHEGAN D. B., *Phys. Rev. Lett.*, **79** (1997) 1572.
- [7] HARILAL S. S., *J. Appl. Phys.*, **102** (2007) 123306.
- [8] AMORUSO S., SAMBRIA A., VITIELLO M. and WANG X., *Appl. Surf. Sci.*, **252** (2006) 4712.
- [9] DIXON R. H. and ELTON R. C., *Phys. Rev. Lett.*, **38** (1977) 1072.
- [10] HARILAL S. S., BIDHU C. V., TILLACK M. S., NAJMABADI F. and GAERIS A. C., *J. Appl. Phys.*, **93** (2003) 2380.

- [11] KOOLS J. C. S., *J. Appl. Phys.*, **74** (1993) 6041.
- [12] HAN M., GONG Y., ZHOU J., YIN C., SONG C. F., MUTO N., TAKIY A. T. and IWATA Y., *Phys. Lett. A.*, **302** (2002) 182.
- [13] WANG Y. L., CHU L. Z., LI Y. L. and FU G. S., *Micro & Nano Lett.*, **4** (2009) 39.
- [14] CIRIMAN M., JOUVARD J. M., LAVISSE L., HALLO L. and OLTRA R., *Appl. Phys. Lett.*, **109** (2011) 103301.
- [15] ZHIGILEI L. V. and GARRISON B. J., *Appl. Phys. Lett.*, **71** (1997) 551.
- [16] YOSHIDA T., TAKEYAMA S., YAMADA Y. and MUTOH K., *Appl. Phys. Lett.*, **68** (1996) 1772.